

Preliminary Study Evaluating the Accuracy of MRI Images on CBCT Images in the Field of Orthodontics

Tai K* / Park JH ** / Hayashi K *** / Yanagi Y **** / Asaumi JI ***** / Iida S ***** / Shin JW *****

Objective: The purpose of this study was to explore the 3-dimensional (3D) accuracy of magnetic resonance imaging (MRI) on cone-beam computed tomography (CBCT) images after the registration of MRI images on CBCT images. **Materials and Methods:** Three Japanese adult females volunteered for this study. To transform digital imaging and communication in medicine (DICOM) data derived from MRI and CBCT images into polygon data, five software programs were used. CBCT and MRI images were obtained within one week, and both were registered by the iterative closest point (ICP) method. To assess the accuracy of the composite MRI-CBCT, the measurement errors of the MRI-CBCT were verified. Measurement values were compared using frontal and cephalometric soft-tissue landmarks. Differences were analyzed using the non-parametric Mann-Whitney U test. **Results:** There were no significant linear measurement errors ($P > 0.05$) when the images were measured from the superimposed MRI-CBCT images. **Conclusion:** The MRI images attained from MRI - CBCT registration showed accurate 3D linear measurements.

Keywords: Magnetic resonance imaging (MRI), cone-beam computed tomography (CBCT), MRI-CBCT registration, 3D accuracy

J Clin Pediatr Dent 36(2): 211–218, 2011

* Kiyoshi Tai, DDS, Visiting Adjunct assistant professor, Postgraduate Orthodontic Program, Arizona School of Dentistry & Oral Health, A.T. Still University, Mesa, AZ, and PhD Program, Department of Oral and Maxillofacial Reconstructive Surgery, Okayama University Graduate School of Medicine, Dentistry and Pharmaceutical Sciences, and Private Practice of Orthodontics, Okayama, Japan.

** Jae Hyun Park, DMD, MSD, MS, PhD, Associate professor and chair, Postgraduate Orthodontic Program, Arizona School of Dentistry & Oral Health, A.T. Still University, Mesa, AZ and International Scholar, the Graduate School of Dentistry, Kyung Hee University, Seoul, Korea.

*** Kunio Hayashi, RT, Central division of radiology Okayama University hospital, Okayama, Japan.

**** Yoshinobu Yanagi, DDS, Senior assistant professor, Department of Oral Diagnosis and Dentomaxillofacial Radiology, Okayama University Hospital, Okayama, Japan.

***** Jun-ichi Asaumi, DDS, DMSci, Professor, Department of Oral and Maxillofacial Radiology, Okayama University Graduate School of Medicine, Dentistry and Pharmaceutical Sciences, Okayama, Japan.

***** Seiji Iida, DDS, PhD, Professor, Department of Oral and Maxillofacial Reconstructive Surgery, Okayama University Graduate School of Medicine, Dentistry and Pharmaceutical Sciences, Okayama, Japan.

***** Je-Won Shin, DMD, MSD, PhD, Professor and chair, Oral Anatomy and Developmental Biology, the Graduate School of Dentistry, Kyung Hee University, Seoul, Korea.

Send all correspondence to Dr. Jae Hyun Park, Postgraduate Orthodontic Program, Arizona School of Dentistry & Oral Health, A.T. Still University, 5835 East Still Circle, Mesa, AZ 85206.

E-mail: JPark@atsu.edu

INTRODUCTION

Digital imaging has become one of the most important diagnostic tools for oral health professionals, and the greatest advance in the past decade has come with the development of cone-beam computed tomography (CBCT). It uses a cone-shaped beam and digital processing to reconstruct a 3-dimensional (3D) image of a patient's complete skull or dental anatomy. In orthodontics, CBCT has been used to augment or replace traditional two-dimensional (2D) radiographs. CBCT imaging has been used in craniofacial abnormalities, cleft lip/palate cases, orthognathic surgery cases, canine impactions, temporomandibular joint (TMJ) evaluations, airway analysis, and root resorption evaluations.¹⁻⁸ Although CBCT images are 3D in nature, traditional 2D views can be created from the CBCT volumes. Numerous studies have shown the validity and reliability of CBCT-derived images.⁹⁻¹⁴

Magnetic resonance imaging (MRI) has been increasingly used for the examination and assessment of various kinds of tissue. Compared with conventional imaging techniques, MRI has several benefits such as the lack of ionizing radiation, low inherent contrast, and multiplanar imaging with no known side effects.^{15,16}

In orthodontics, to image the TMJ, jaw muscles, and faces of patients with jaw deformity, MRI has become an important diagnostic instrument.¹⁷ If MRI can provide satisfactory image quality for both jaws, including TMJ and soft tissues, it might be possible to obtain diagnostic imaging information from MRI.

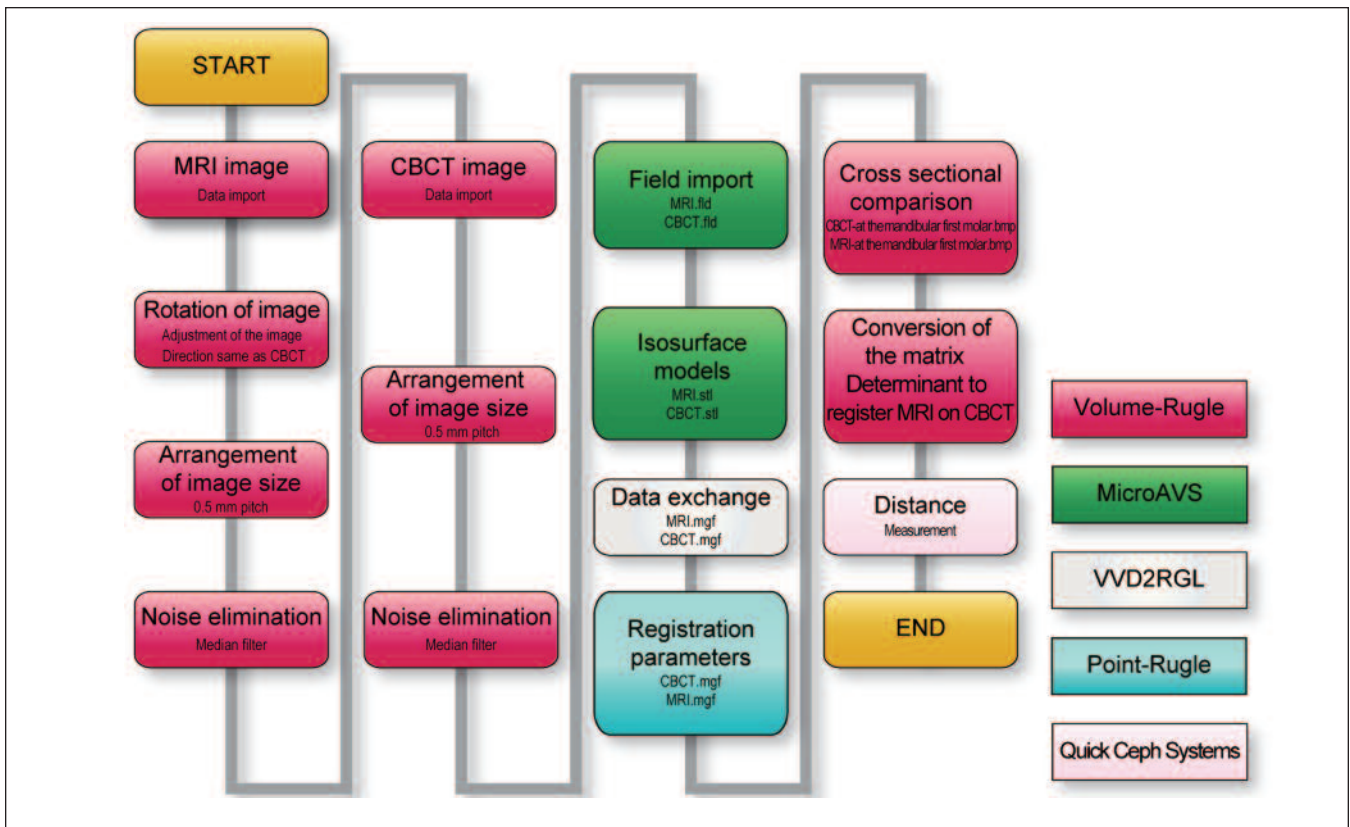


Figure 1. A flow chart showing the methods used to convert CBCT/MRI-derived DICOM data into polygon data. For registration the polygon data was used, and the Quick Ceph Systems software was used for measuring the target distances.

The purpose of this study was to explore the dimensional accuracy of MRI images after the image registration and fusion of CBCT and MRI using different software programs.

MATERIALS AND METHOD

The study was approved by the ethics committee of Okayama University Graduate School of Medicine, Dentistry and Pharmaceutical Sciences. Three adult Japanese females with an average age of 32 years 2 months old, volunteered for the study and an informed consent was obtained from the participants.

Five different software programs, Volume-Rugle (Medic Engineering, Kyoto, Japan), MicroAVS (KGT, Tokyo, Japan), VVD2RGL (Medic Engineering, Kyoto, Japan), Point-Rugle (Medic Engineering, Kyoto, Japan), Quick Ceph Systems (Quick Ceph Systems, Inc. San Diego, Calif) were used to transform the digital imaging and communication in medicine (DICOM) data from MRI and CBCT images into polygon data respectively (Figure 1).

It is possible to very precisely superimpose images with good repeatability with the iterative closest point (ICP) method because numerous corresponding points are utilized to compare with point-based registration.¹⁸⁻²⁰ Therefore, the ICP method was used to superimpose two 3D CBCT and MRI images.

The T-zone of the forehead, nose, and chin were used as reference points²¹ for registration (superimposition) to enhance the accuracy of the ICP method (Figure 2).



Figure 2. The T-zone of the forehead, nose, and chin were used as reference points for registration (superimposition) to enhance the accuracy of the ICP method. The green and gray colors represented CBCT and MRI images respectively.

The multiplanar reconstruction (MPR) images, which display excellent dimensional accuracy,²² were used to compare the MRI and CBCT data. After registration, the

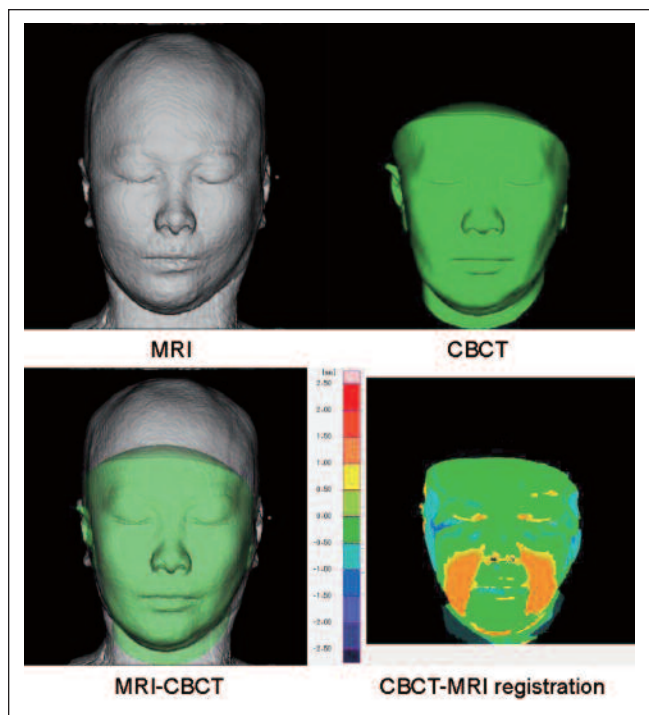


Figure 3. CBCT-MRI superimposition and registration. The pale green area shows that superposition (or registration) was performed within ± 0.50 mm. The yellow area shows it to range from $+0.50$ mm to $+1.00$ mm. The light blue area shows it to range from -0.50 mm to -1.00 mm.

combined MRI and CBCT images were sectioned on an arbitrary plane and converted into two units. This method makes an accurate superimposition of two separate MPR images possible (Figures 3 and 4).

The Quick Ceph Systems was used for each measurement. A measurement error test was done to validate the superimposition technique and analysis of the MPR images after superimposing the CBCT and MRI 3D images to confirm the absence of processing errors during data conversion of the images.

A natural head position²³ was obtained by orienting the Frankfurt plane parallel to the floor with the subject in a seated position, and an image was taken at the intercuspal position using a CB MercurRay (Hitachi Medical Corporation, Tokyo, Japan). The MR examination was performed on a 1.5 T unit (Magnetom Vision; Siemens, Erlangen, Germany) with a head-neck coil, and an image was taken at the intercuspal position with the patient lying in a supine position.

CBCT images and MRI images of the subjects were taken separately (within a 1 week period), and the registration was performed by the ICP technique for superimposition.^{24,25}

The direction of the CBCT was adjusted to match the MRI direction because the X, Y, and Z directions of the MRI and CBCT images were different. The different voxel sizes of CBCT and MRI was unified to 0.5 mm to facilitate superimposition.

Before the MRI and CBCT images were resized, the X, Y, and Z vector coordinates were specified respectively.

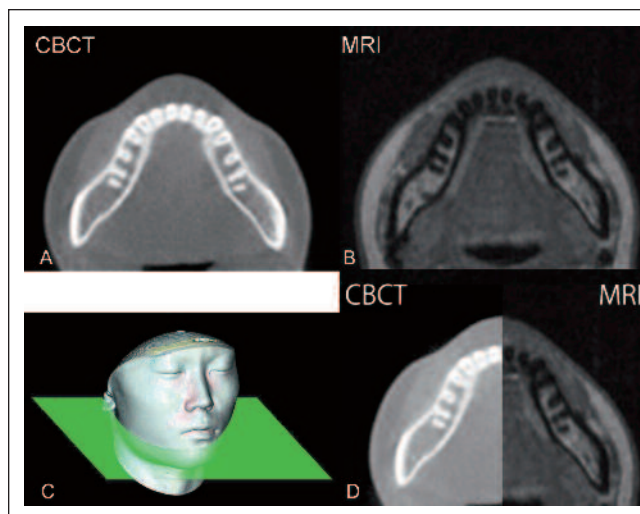


Figure 4. Two representative images of CBCT (A) and MRI (B). The combined MRI/CBCT images are obtained from the same cross-section (C and D).

After resizing, the coordinate system was assigned to the corresponding superimposition.

The distances between landmarks were measured on the composite MPR images using the Quick Ceph Systems after superimposition of MRI on CBCT and the two fused 3D images were sectioned on an arbitrary plane. The MPR images, which display excellent dimensional accuracy,²² were used to compare the MRI and CBCT data.

Verification of measurement error using dental casts

The distance between the actual landmarks on the dental casts from the 3 volunteers were measured using a digital caliper (NTD 12-15PMX, Mitsutoyo, Kanagawa, Japan), which is accurate to 0.01 mm. The landmarks and their characteristics used in this study are listed (Figure 5 and Table I).

Table I. The investigated distances on study models

Landmarks for parameter	Measured landmarks
1. UR3-UL3 (transverse)	The distance between the maxillary canine cusp tips
2. UR6 _{CEJ} -UL6 _{CEJ} (transverse)	The distance between the maxillary first molars at the middle of palatal cervical margin
3. LR3-LL3 (transverse)	The distance between the mandibular canine cusp tips
4. LR6 _{CEJ} -LL6 _{CEJ} (transverse)	The distance between the mandibular first molars at the CEJ
5. U1center-U6mesial (sagittal)	The distance from the mesial contact point of the maxillary central incisors to a line connecting the mesial contacts of the maxillary first molars
6. L1center-L6mesial (sagittal)	The distance from the mesial contact point of the mandibular central incisors to a line connecting the mesial contacts of the mandibular first molars
7. UR3 _{CEJ} -LR3 _{CEJ} (vertical)	The distance between the CEJ of the maxillary and mandibular right canines
8. UL3 _{CEJ} -LL3 _{CEJ} (vertical)	The distance between the CEJ of the maxillary and mandibular left canines

CEJ, Cementoenamel junction.

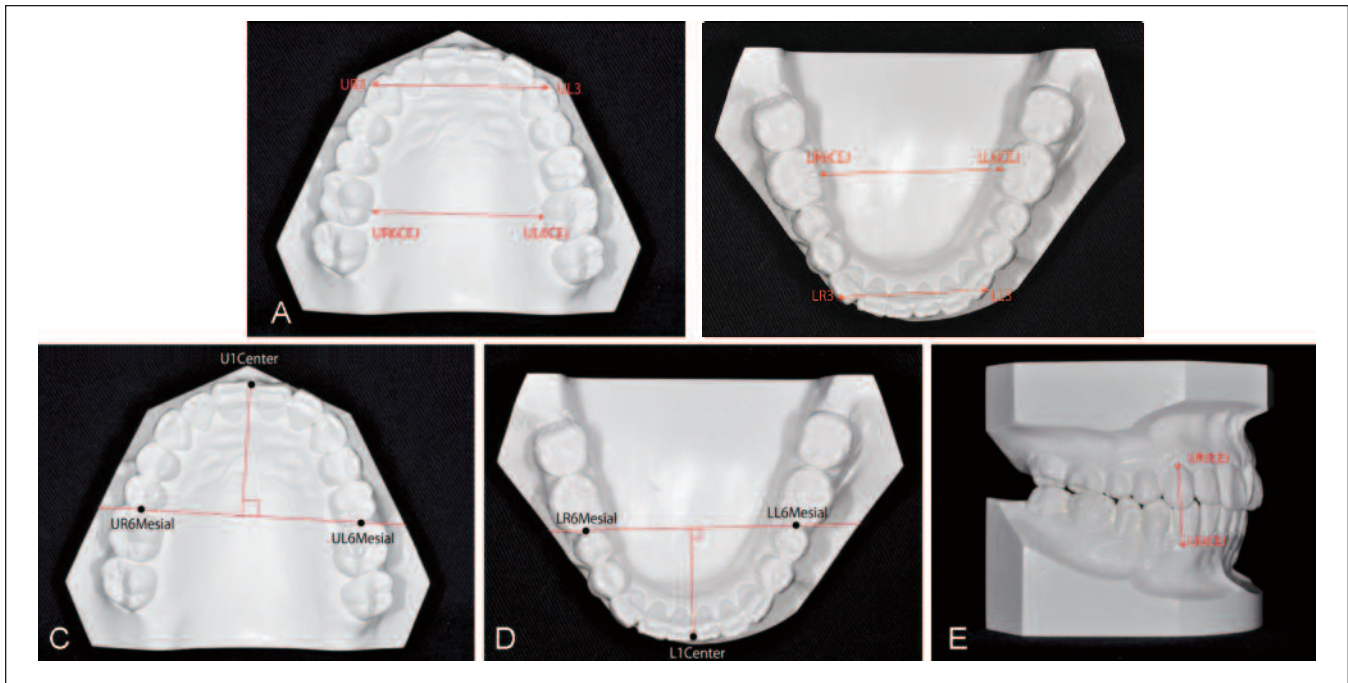


Figure 5. Linear measurements on study models. A and B, transverse; C and D, sagittal; E, vertical.

The same points on the dental casts were measured from the MRI and CBCT data after superimposition and compared with direct measurement.

Verification of measurement error using soft tissue anatomical landmarks

Seven soft tissue linear measurements were performed respectively from the MRI and CBCT data after superimposition by using the Quick Ceph Systems (Figure 6).

Measurement Errors

One observer (KT) performed 10 independent measure-

ments of the distances between the landmarks to eliminate inter-examiner errors. Their average and standard deviation were calculated, followed by an analysis of the significance. The standard deviation (SD) of each measurement was compared to voxel size to confirm the reliability of each measuring method.¹⁷

The differences (mm) between measurements from direct osteometry using dental casts and 3D distances on MRI or CBCT were examined. Measurement accuracy, expressed as the relative errors (%), was calculated with respect to the measured real lengths using direct osteometry to confirm the reliability of image quality.

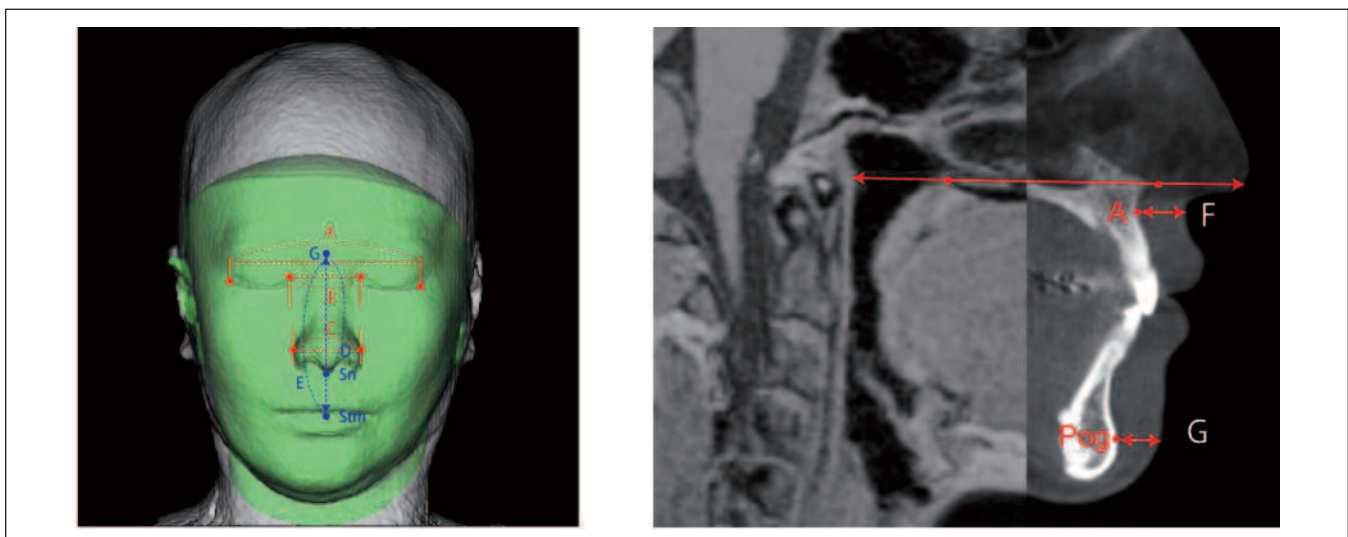


Figure 6. Soft-tissue landmarks used in this study. A (Ex-width), the distance between the right and left exocantion; B (En-width), the distance between the right and left endocantion; C (Ab-width), the distance between the right and left alar base; D (G'-Sn), the distance between the soft tissue glabella and subnasale; E (G'-Stm), the distance between the soft tissue glabella and stomion; F (upper lip thickness), the distance between point A to the outer border of the upper lip; G (Soft-tissue-chin thickness), the distance between pogonion and the most prominent point on the chin.

To identify systematic errors and to compare measurement accuracy, intra-examiner reliability was evaluated. Sources of error included landmark location, data conversion from different software programs, and all linear measurements from the MRI and CBCT. The data conversion errors from different software programs, and linear measurement error of MRI and CBCT, as well as all linear measurements were determined by performing each measurement twice on two separate occasions, 4 weeks apart. 4 randomly selected data from MRI and CBCT (after superimposition of MRI on CBCT) were measured twice on two separate occasions, 4 weeks apart, by the same investigator. No statistically significant difference was found in any measurement by using the intraclass correlation coefficients (ICC).²⁶

Descriptive statistics were calculated for each measurement. The data were analyzed using a statistical software package (SPSS version 16.0) and the Mann-Whitney U-test was used to analyze any difference in the measurement. A value of $P < 0.05$ was considered to indicate significance.

RESULTS

Verification of measurement error using dental casts

The linear measurements of the dental cast using CBCT and MRI images were quantified. These errors included any differences generated during the software data conversion. The margin of error and average error rates measurements ranged from $\pm 0.29 - 0.71$ mm and $0.95 - 2.44\%$ respectively. There were no significant differences ($P > 0.05$) compared with the direct measurement (Table II).

Verification of measurement error using soft tissue anatomical landmarks

The mean differences of the anatomical landmarks of the soft tissue measurements from CBCT and MRI scans after superimposition of both images ranged from -0.60 to 0.73 mm. When comparing the 2 observed measurements between 2 scans, no statistically significant difference ($P > 0.05$) was found between any of the 3D linear measurements (Table III).

Table II. The verification of measurement errors using MPR images and cast models

Landmarks for parameter	Mean (mm)	SD	Margin of error (mm)			Rate of average error (%)		
			A-B	B-C	A-C	A-B	B-C	A-C
UR3-UL3 (transverse)	35.72	6.73	± 0.58	± 0.42	± 0.34	1.62	1.18	0.95
UR6 _{CEJ} -UL6 _{CEJ} (transverse)	36.06	6.04	± 0.63	± 0.51	± 0.46	1.75	1.41	1.28
LR3-LL3 (transverse)	29.61	4.46	± 0.53	± 0.43	± 0.29	1.79	1.45	0.98
LR6 _{CEJ} -LL6 _{CEJ} (transverse)	38.22	4.34	± 0.71	± 0.39	± 0.41	1.86	1.02	1.07
U1center-U6mesial (sagittal)	27.83	5.77	± 0.59	± 0.48	± 0.45	2.12	1.72	1.62
L1center-L6mesial (sagittal)	23.74	5.19	± 0.49	± 0.48	± 0.49	2.06	2.02	2.02
UR3 _{CEJ} -LR3 _{CEJ} (vertical)	18.48	3.67	± 0.45	± 0.43	± 0.42	2.44	2.33	2.27
UL3 _{CEJ} -LL3 _{CEJ} (vertical)	17.17	3.83	± 0.41	± 0.38	± 0.35	2.39	2.21	2.04

A: the distance measured on the MPR image of CBCT after superimposition of MRI on CBCT using the Quick Ceph Systems, B: the same distances on the MPR image of MRI after superimposition of MRI on CBCT using the Quick Ceph Systems, C: the same distances of the model cast measured manually using a digital caliper.

Table III. Changes in orientation during scanning of soft-tissue after superimposition

Distances	CBCT		MRI		Mean difference (mm)	P value
	Mean (mm)	SD	Mean (mm)	SD		
Transverse						
Ex-width	101.15	25.98	101.88	31.87	0.73	.34
En-width	34.66	7.79	34.98	12.35	0.32	.55
Ab-width	37.65	8.02	37.25	13.37	-0.39	.66
Vertical						
G'-Sn	93.37	26.21	92.77	28.46	-0.60	.78
G'-Stm	74.51	16.64	74.51	21.49	0.81	.29
Sagittal						
Upper lip thickness	1.54	0.69	1.73	0.94	0.19	.28
Soft-tissue-chin thickness	1.32	0.75	1.14	0.87	-0.18	.53

Ex-width, the distance between the right and left exocantion; En-width, the distance between the right and left endocantion; Ab-width, the distance between the right and left alar base; G'-Sn, the distance between the soft-tissue glabella and subnasale; G'-Stm, the distance between the soft-tissue glabella and stomion; Upper lip thickness, the distance between point A to the outer border of the upper lip; Soft-tissue-chin thickness, the distance between pogonion and the most prominent point on the chin.

DISCUSSION

MRI is an essential diagnostic tool in both medicine and dentistry and MRI images offer several advantages over conventional imaging modalities. MRI does not pose a risk from ionizing radiation, is excellent for imaging tissues with low inherent contrast, and allows MPR images without moving the patient.²⁷

The main goal of this study was to determine whether MRI could be added to CBCT as a useful orthodontic diagnostic procedure. Several studies have reported on the accuracy of CT, CBCT and MRI,^{17,28,29} but no previous reports have reported on their accuracy following superimposition. To fill this gap, we compared CBCT and MRI measurements with direct measurements after CBCT-MRI superimpositions (matching). The accuracy of superimposition was evaluated on both dental cast measurements and soft-tissue landmarks. After superimposition there was no statistically significant difference ($P > 0.05$) between CBCT-caliper, MRI-caliper, CBCT-MRI measurements on dental casts, as well as in CBCT-MRI of the soft-tissue landmarks.

Because the soft tissues change with growth, treatment, facial expression, head posture, weight change, and aging, soft-tissue structures are not stable enough to allow registration between pre- and posttreatment images. However, the ability to distinguish fat and other soft tissues in living subjects has progressed remarkably with MRI. MRI has superior soft-tissue contrast compared to that of CT and several studies have reported the advantages of utilizing MR images for delineation of soft-tissue.³⁰⁻³² The precision of MRI in differentiating the components of facial soft-tissues makes it a versatile tool for quantitative study of changes of the face.³³

The current study investigated using MRI in the evaluation of facial soft tissues by utilizing MPR images following the image registration and merging of CBCT and MRI from various program packages. The results of the study presented precise resolution of the facial tissue planes, muscles, fascial septa, fat and skin. However, some extent of partial volume effect was observed in the volume rendering MRI images (Minimum unit volumes of MRI and CBCT could not be differentiated, which worsened with increases in slice thickness.) as a result of discrepancy in voxel sizes between MRI (1.0 mm) and CBCT (0.29 mm). Even if the surface quality of MRI was not as high as CBCT, it had no effect on precision since MPR image of MRI presented correct dimensions.

In this study precision of MRI was investigated with various software packages used as measurement methods. Our findings show that once pixel sizes were converted into common dimensions, Quick Ceph Systems could be replaced with other programs, such as Dolphin Imaging (Dolphin Imaging systems, Chatsworth, Calif) to measure distances after registration.

With the application of MRI, there are some issues that need to be further addressed, such as spatial distortions,

which tend to be higher than those presented by CT scans, and might become a limiting factor in a practical application. Another concern is related to the materials used, such as wires and brackets. Creation of magnetic fields by MRI produces artifacts due to the magnetic susceptibility effect.³⁴ Ferromagnetic materials and some metals and alloys such as nickel, lead and chrome obstruct the signal by changing the homogeneity of the magnetic field, causing problems with reconstruction of MRI images.^{35,36} Obstruction of the signal and the distortion caused by the presence of stainless steel brackets is so strong that it makes rendering of close cranial regions impossible. Silver alloys cause less image distortion.³⁷ If MRI is to be used for mid treatment measurements, selection of the type of fixed orthodontic appliances should be made accordingly. As reported by Elison *et al*³⁸ titanium, plastic and ceramic brackets cause minimal distortion of cranial MRI images.

Our preliminary results are encouraging, but it is obvious that application of MRI for orthodontic diagnostic purposes will require more research in the future. There were several limitations in our study. First, our sample was relatively small and included only 3 subjects. Further studies on a larger sample group with different anatomical landmarks combined with linear and angular measurements by different examiners are recommended.

As with every other method and device, MRI has some potential downsides including high cost, restricted availability, concern for claustrophobic patients, magnetic safety concerns, detection of calcifications and cortical bone contrast which is not ideal.

In order to evaluate MRI's value as a prospective orthodontic diagnostic tool, and to determine whether its potential could be developed to the point where it might become the new golden standard in imaging, further studies should be conducted. Proper MRI imaging settings need to be identified and distortion issues need to be resolved before MRI can be considered for wide use in orthodontic treatment planning. The establishment of precise methods for registration, image segmentation and correlation is necessary to secure precise, punctual, repeatable MRI data.³⁹ Furthermore, clinical studies comparing it with CBCT and addressing the cost-benefit relationship should be conducted to evaluate MRI's value in clinical treatment planning.

CONCLUSIONS

Because CBCT and MRI provide complementary data, the fused images of CBCT and MRI could be utilized for accurate diagnosis and treatment planning. To observe not only soft tissue, but also hard tissue, MRI data could be a useful armamentarium. We were able to validate the accuracy of registration between MRI and CBCT. The MPR images obtained from this registration showed excellent dimensional accuracy.

REFERENCES

1. Terajima M, Nakasima A, Aoki Y, Goto TK, Tokumori K, Mori N, Hoshinod Y. A 3-dimensional method for analyzing the morphology of patients with maxillofacial deformities. *Am J Orthod Dentofacial Orthop*, 136: 857–867, 2009.
2. Oberoi S, Chigurupati R, Gill P, Hoffman WY, Vargervik K. Volumetric assessment of secondary alveolar bone grafting using cone beam computed tomography. *Cleft Palate Craniofac J*, 46: 503–511, 2009.
3. Carvalho FDAR, Cevidanes LHS, da Motta ATS, Almeida MADO, Phillips C. Three-dimensional assessment of mandibular advancement 1 year after surgery. *Am J Orthod Dentofacial Orthop*, 137: S53.e1–e12, 2010.
4. Haney E, Gansky SA, Lee JS, Johnson E, Maki K, Miller AJ, Huang JC. Comparative analysis of traditional radiographs and cone-beam computed tomography volumetric images in the diagnosis and treatment planning of maxillary impacted canines. *Am J Orthod Dentofacial Orthop*, 137: 590–597, 2010.
5. Honey OB, Scarfe WC, Hilgers MJ, Klueber K, Silveira AM, Haskell BS, Farman AG. Accuracy of cone-beam computed tomography imaging of the temporomandibular joint: comparisons with panoramic radiology and linear tomography. *Am J Orthod Dentofacial Orthop*, 132: 429–438, 2007.
6. Hilgers ML, Scarfe WC, Scheetz JP, Farman AG. Accuracy of linear temporomandibular joint measurements with cone beam computed tomography and digital cephalometric radiography. *Am J Orthod Dentofacial Orthop*, 128: 803–811, 2005.
7. Kim Y, Hong J, Hwang Y, Park Y. Three-dimensional analysis of pharyngeal airway in preadolescent children with different anteroposterior skeletal patterns. *Am J Orthod Dentofacial Orthop*, 137: 306.e1–e11, 2010.
8. Liu D, Zhang W, Zhang Z, Wu Y, Ma X. Localization of impacted maxillary canines and observation of adjacent incisor resorption with cone-beam computed tomography. *Oral Surg Oral Med Oral Pathol Oral Radiol Endod*, 105: 91–98, 2008.
9. Berco M, Rigali PH, Miner RM, DeLuca S, Anderson NK, Will LA. Accuracy and reliability of linear cephalometric measurements from cone-beam computed tomography scans of a dry human skull. *Am J Orthod Dentofacial Orthop*, 136: 17.e1–e9, 2009.
10. Moshiri M, Scarfe WC, Hilgers ML, Scheetz JP, Silveira AM, Farman AG. Accuracy of linear measurements from imaging plate and lateral cephalometric images derived from cone-beam computed tomography. *Am J Orthod Dentofacial Orthop*, 132: 550–560, 2007.
11. Oliveira AE, Cevidanes LH, Phillips C, Motta A, Burke B, Tyndall D. Observer reliability of three-dimensional cephalometric landmark identification on cone-beam computerized tomography. *Oral Surg Oral Med Oral Pathol Oral Radiol Endod*, 107: 256–265, 2009.
12. van Vlijmen O, Bergé S, Swennen G, Bronkhorst EM, Katsaros C, Kuijpers-Jagtman AM. Comparison of cephalometric radiographs obtained from cone-beam computed tomography scans and conventional radiographs. *J Oral Maxillofac Surg*, 67: 92–97, 2009.
13. Chien PC, Parks ET, Eraso F, Hartsfield JK, Roberts WE, Ofner S. Comparison of reliability in anatomical landmark identification using two-dimensional digital cephalometrics and three-dimensional cone beam computed tomography in vivo. *Dentomaxillofac Radiol*, 38: 262–273, 2009.
14. Lamichane M, Anderson NK, Rigali PH, Seldin EB, Will LA. Accuracy of reconstructed images from cone-beam computed tomography scans. *Am J Orthod Dentofacial Orthop*, 136: 156.e1–e6, 2009.
15. Tasaki MM, Westesson PL. Temporomandibular joint: diagnostic accuracy with sagittal and coronal MR imaging. *Radiology*, 186: 723–729, 1993.
16. Tasaki MM, Westesson PL, Isberg AM, Ren YF, Tallents RH. Classification and prevalence of temporomandibular joint disk displacement in patients and symptom-free volunteers. *Am J Orthod Dentofacial Orthop*, 109: 249–262, 1996.
17. Goto TK, Nishida S, Nakamura Y, Tokumori K, Nakamura Y, Kobayashi K, Yoshida Y, Yoshiura K. The accuracy of 3-dimensional magnetic resonance 3D vibe images of the mandible: an in vitro comparison of magnetic resonance imaging and computed tomography. *Oral Surg Oral Med Oral Pathol Oral Radiol Endod*, 103: 550–559, 2007.
18. Horn BKP. Closed-form solution of absolute orientation using unit quaternions. *J Opt Soc of Am*, 44: 629–642, 1987.
19. Arun KS, Huang TS, Blostein SD. Least-squares fitting of two 3-dimensional point sets. *IEEE Trans Pattern Anal Mach Intell*, 9: 698–700, 1987.
20. Declercq J, Feldmar J, Goris ML. Automatic registration and alignment on a template of cardiac stress and rest reoriented SPECT images. *IEEE Trans Med Imaging*, 16: 727–737, 1997.
21. Terajima M, Furuichi Y, Aoki Y, Goto TK, Tokumori K, Nakasima A. A 3-dimensional method for analyzing facial soft-tissue morphology of patients with jaw deformities. *Am J Orthod Dentofacial Orthop*, 135: 715–722, 2009.
22. Kataoka Y, Nakano H, Matsuda Y, Araki K, Okano T, Maki K. Three dimensional diagnostic imaging of the alveolar bone using dento-maxillofacial cone beam X-ray CT. *Orthod Waves-Jpn Ed*, 66: 81–91, 2007.
23. Moorrees CFA. Natural head position—a revival. *Am J Orthod Dentofacial Orthop*, 105: 512–513, 1994.
24. Tai K, Hotokezaka H, Park JH, Tai H, Miyajima K, Choi M, et al. Preliminary cone-beam computed tomography study evaluating dental and skeletal changes after treatment with a mandibular Schwarz appliance. *Am J Orthod Dentofacial Orthop*, 138: 262.e1–e11, 2010.
25. Tai K, Park JH, Mishima K, Hotokezaka H. Using superimposition of 3-dimensional cone-beam computed tomography images with surface-based registration in growing patients. *J Clin Pediatr Dent*, 34: 361–368, 2010.
26. Bravo G, Potvin L. Estimating the reliability of continuous measures with Cronbach’s alpha or the intraclass correlation coefficient: toward the integration of two traditions. *J Clin Epidemiol*, 44: 381–390, 1991.
27. White SC, Pharoah MJ. *Oral radiology: principles and interpretation*. 4th ed. Mosby, St Louis; 2000.
28. Wyper DJ, Turner JW, Patterson J, Condon BR, Grossart KW, Jenkins A, et al. Accuracy of stereotaxic localization using MRI and CT. *J Neurol Neurosurg Psychiatry*, 49: 1445–1448, 1986.
29. Buhl SK, Duun-Christensen AK, Kristensen BH, Behrens CF. Clinical evaluation of 3D/3D MRI-CBCT automatching on brain tumors for online patient setup verification – A step towards MRI-based treatment planning. *Acta Oncologica*, 49: 1085–1091, 2010.
30. Weltens C, Menten J, Feron M, Bellon E, Demaerel P, Maes F, et al. Interobserver variations in gross tumor volume delineation of brain tumors on computed tomography and impact of magnetic resonance imaging. *Radiother Oncol*, 60: 49–59, 2001.
31. Rasch C, Barillot I, Remeijer P, Touw A, van Herk M, Lebesque JV. Definition of the prostate in CT and MRI: a multi-observer study. *Int J Radiat Oncol Biol Phys*, 43: 57–66, 1999.
32. Khoo VS, Dearnaley DP, Finnigan DJ, Padhani A, Tanner SF, Leach MO. Magnetic resonance imaging (MRI): Considerations and applications in radiotherapy treatment planning. *Radiother Oncol*, 42: 1–15, 1997.
33. Gosain AK, Amarante MTJ, Hyde JS, Yousif N. A dynamic analysis of changes in the nasolabial fold using magnetic resonance imaging: implications for facial rejuvenation and facial animation surgery. *Plastic & Reconstructive Surgery*, 98: 622–636, 1996.
34. Beuf O, Lissac M, Cremillieux Y, Briguet A. Correlation between magnetic resonance imaging disturbances and the magnetic susceptibility of dental materials. *Dent Mater*, 10: 265–268, 1994.
35. Brown B, Swallow C, Eiseman A. MRI artifact masquerading as orbital disease. *Int Ophthalmol*, 24: 343–347, 2001.
36. Lissac M, Coudert JL, Briguet A, Amiel M. Disturbances caused by dental materials in magnetic resonance imaging. *Int Dent J*, 42: 229–233, 1992.

37. Heindel W, Friedman G, Bunke J, Thomas B, Firsching R, Ernestus RI. Artifacts in MR imaging after surgical intervention. *J Comput Assist Tomogr*, 10: 596–599, 1986.
38. Elison JM, Leggitt VL, Thomson M, Oyoyo U, Wycliffe ND. Influence of common orthodontic appliances on the diagnostic quality of cranial magnetic resonance images. *Am J Orthod Dentofacial Orthop*, 134: 563–572, 2008.
39. Khoo VS, Dearnaley DP, Finnigan DJ, Padhani A, Tanner SF, Leach MO. Magnetic resonance imaging (MRI): Considerations and applications in radiotherapy treatment planning. *Radiother Oncol*, 42: 1–15, 1997.